REPORT DOCUMENTATION PAGE

Public reporting burden for this collection of information is estimated to average 1 hour per response, including the time for reviewing instructions, searching existing data sources, gathering and maintaining the data needed, and completing and reviewing this collection of information. Send comments regarding this burden estimate or any other aspect of this collection of information, including suggestions for reducing this burden to Department of Defense, Washington Headquarters Services, Directorate for Information Operations and Reports (0704-0188), 1215 Jefferson Davis Highway, Suite 1204, Arlington, VA 22202-4302. Respondents should be aware that notwithstanding any other provision of law, no person shall be subject to any penalty for failing to comply with a collection of information if it does not display a currently valid OMB control number. **PLEASE DO NOT RETURN YOUR FORM TO THE ABOVE ADDRESS.**

1. REPORT DATE *(DD-MM-YYYY)* 08-03-2006	2. REPORT TYPE Technical Paper	3. DATES COVERED *(From - To)*

4. TITLE AND SUBTITLE **Atomization in Gas-Centered Swirl-Coaxial Injectors (POSTPRINT)**	5a. CONTRACT NUMBER
	5b. GRANT NUMBER
	5c. PROGRAM ELEMENT NUMBER
6. AUTHOR(S) M.D.A. Lightfoot, S.A. Danczyk, & D.G. Talley (AFRL/PRSA)	5d. PROJECT NUMBER 50260548
	5e. TASK NUMBER
	5f. WORK UNIT NUMBER

7. PERFORMING ORGANIZATION NAME(S) AND ADDRESS(ES) Air Force Research Laboratory (AFMC) AFRL/PRSA 10 E. Saturn Blvd. Edwards AFB CA 93524-7680	8. PERFORMING ORGANIZATION REPORT NUMBER AFRL-PR-ED-TP-2006-088

9. SPONSORING / MONITORING AGENCY NAME(S) AND ADDRESS(ES) Air Force Research Laboratory (AFMC) AFRL/PRS 5 Pollux Drive Edwards AFB CA 93524-70448	10. SPONSOR/MONITOR'S ACRONYM(S)
	11. SPONSOR/MONITOR'S NUMBER(S) AFRL-PR-ED-TP-2006-088

12. DISTRIBUTION / AVAILABILITY STATEMENT

Approved for public release; distribution unlimited (AFRL-ERS-PAS-2006-073)

13. SUPPLEMENTARY NOTES
Presented at the Institute for Liquid Atomization and Spray Systems (ILASS) – Americas Meeting, Toronto, Canada, 23-26 May 2006.

14. ABSTRACT
        A preliminary study of atomization mechanisms in gas-centered swirl-coaxial injectors for use in rocket engines has been undertaken. Gas-centered swirl-coaxial injectors differ from other injectors in that atomization occurs from a wall-bounded liquid. Few studies of atomization mechanisms in wall-bounded flows exist; some probable atomization processes have been determined, however. These mechanisms include liquid turbulence, aerodynamic stripping and a process driven by gas-phase structures. The likely character of the gas and film undergoing these atomization processes is presented. Relevant nondimensional groupings based on simplified theoretical descriptions of select mechanisms are outlined. Preliminary experimental and numerical results taken at atmospheric pressure are qualitatively compared to the likely mechanisms and each other.

15. SUBJECT TERMS

16. SECURITY CLASSIFICATION OF:			17. LIMITATION OF ABSTRACT	18. NUMBER OF PAGES	19a. NAME OF RESPONSIBLE PERSON Dr. Douglas G. Talley
a. REPORT **Unclassified**	b. ABSTRACT **Unclassified**	c. THIS PAGE **Unclassified**	A	12	19b. TELEPHONE NUMBER *(include area code)* N/A

Atomization in Gas-Centered Swirl-Coaxial Injectors

M.D.A. Lightfoot[*], S.A. Danczyk and D.G. Talley
Air Force Research Laboratory
Edwards Air Force Base
Edwards AFB, CA 93524-7660 USA

Abstract

A preliminary study of atomization mechanisms in gas-centered swirl-coaxial injectors for use in rocket engines has been undertaken. Gas-centered swirl-coaxial injectors differ from other injectors in that atomization occurs from a wall-bounded liquid. Few studies of atomization mechanisms in wall-bounded flows exist; some probable atomization processes have been determined, however. These mechanisms include liquid turbulence, aerodynamic stripping and a process driven by gas-phase structures. The likely character of the gas and film undergoing these atomization processes is presented. Relevant nondimensional groupings based on simplified theoretical descriptions of select mechanisms are outlined. Preliminary experimental and numerical results taken at atmospheric pressure are qualitatively compared to the likely mechanisms and each other.

[*]Corresponding author

Introduction

Recently, gas-centered swirl-coaxial (GCSC) injectors have garnered attention for use in rocket engines [1, 2]. These injectors operate like pressure-swirl atomizers with the addition of gas flow. A schematic of the injector is shown in Fig. 1. Liquid moves from a plenum to the outer wall of the injectors where it is injected tangentially. As a result of the tangential injection the liquid rotates about the axis of the injector forming a swirling film along the wall. Gas is introduced axially through the center of this swirling flow. The large aerodynamic forces make this injector an effective atomizer [2]. GCSC injectors have several advantages over more traditional designs including the ability to decouple the fuel feed system from any variations in chamber pressure [3]. Design strategies for these injectors remain poorly understood, however, because their operation differs from the more common injectors which they superficially resemble, i.e. pressure-swirl and coaxial air-blast atomizers. At their standard operating conditions in rockets GCSC injectors do not produce a conical sheet, as the more common injectors do, an obvious departure from other injectors. Atomization occurs within the injector cup instead [2]. In other words, droplets are produced by a wall-bounded film, not from the more frequently encountered sheet or jet.
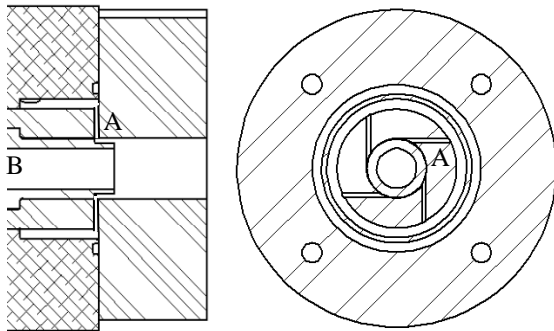

Figure 1. Partial schematic of the experimental apparatus. The liquid enters through the tubes labeled A; gas enters at B. The gas inlet extends beyond what is pictured.

A more thorough understanding of the film atomization process must be developed to enable the characterization and improvement of GCSC injectors. Part of developing this understanding involves determining the underlying causes, or mechanisms, of atomization from wall-bounded films. A recent literature review conducted by the authors identifies a variety of potential mechanisms, but concludes that there are three most-likely culprits: liquid turbulence, stripping of waves generated by hydrodynamic instabilities and behavior related to vortices in the gas-phase [6]. The first two of these have been observed in flat films under differing inlet conditions [4, 7, 8]. The third was observed during recent studies and is reported on herein. Each has been observed (seemingly) on their own, so there appear to be at least three modes of film atomization. To properly predict atomizer performance one must know the mode in which the atomizer operates. Additionally, knowledge of the design parameters relevant to the operating mode is necessary in order to design efficient and effective injectors.

In order to advance the understanding of GCSC injectors and film atomization in general a series of experiments and numerical simulations are being undertaken. This paper outlines these activities and reports some preliminary findings. The following section discusses the three modes of film atomization including the likely relevant design parameters. Subsequent to this introductory description the setup for the numerical simulations and experiments is given. The initial results of both the simulations and experiments are presented in the Results and Discussion section.

Film Atomization Regimes

Studies have suggested three causes of atomization from wall-bounded films: liquid turbulence, stripping of waves and stripping/tearing resulting from gas-phase vortices [6]. These three mechanisms produce different droplet sizes and proceed at different rates so that they constitute three different atomization behaviors. The three are not exclusive, that is multiple mechanisms may be operable at the same time, but there will be regimes in which one is dominant over the others. To properly design an atomizer the operating mode must be known. Prior to determining the bounding conditions for these modes, a better understanding of each mechanism is required.

Turbulent eddies within the liquid can interact with the interface causing it to become roughened and eventually forming ligaments. These ligaments may then break down into droplets, generally via a Rayleigh breakup mechanism. These events have been observed in flat and annular films exiting into quiescent environments [4, 8]. Characteristic features include roughly cylindrical surface projections; this mode may be differentiated from others by the chaotic distribution and relatively narrow width of the surface disturbances. Dai et al. [8] give estimates of the length required for the onset of atomization as well as other atomization parameters based on arguments involving the energy and size of the eddies. They neglect aerodynamic forces in their formulation due to the low ratio of air-to-liquid densities and the lack of imposed flow in the gas-phase. Their results cite several important nondimensional parameters including ratios of film height to hydraulic diameter and mean velocity to rms velocity fluctuations as well as a liquid Weber number based on hydraulic diameter and mean surface velocity. In the

absence of important aerodynamic forces, liquid turbulence will be important when the liquid Reynolds number is sufficiently large for the film to be turbulent (i.e, Re>2300) assuming the film length is sufficient to allow the growth of the turbulent boundary layer.

If aerodynamic forces are important the character of the interface will be different. As the forces increase fewer ligaments will be formed and less of these will undergo Rayleigh breakup. Eventually, behavior caused by the aerodynamic forces will become dominant over any behavior caused by liquid turbulence.

When aerodynamics are important two different types of surface distortions may appear—hydrodynamic instabilities, e.g. Kelvin-Helmholtz instabilities, and interface distortions due to gas-phase structures such as a vortex formed as gas passes a backward facing step. Hydrodynamic instabilities have been the focus of much atomization literature, especially in relation to pressure-swirl atomizers [9, for example]. Instabilities may arise due to differences in velocities, densities, viscosities, etc. of the two fluids. These instabilities cause waves to form and grow on the interface between the gas and liquid. Aerodynamic forces may augment the growth of these waves and lead to droplet formation by stripping mass from the wave crest. Much literature has addressed the conditions for which a film/sheet will form waves and the reader is referred to this body of work for more details on parameters which describe film instabilities [9, for example].

Because the film is bounded by a wall, the growth of these waves alone does not guarantee atomization as it does in a sheet. However, the acceleration of air over the waves not only enhances their growth but also can separate mass from their crests. This separation was observed by Woodmansee and Hanratty [7] in their studies of flat films. They assumed a pressure differential over the curved surface led to mass being "pulled" from the waves. Their analysis indicates the ratio of wave height to film length or gas space and a sort of gas Weber number based on film length and the relative velocity between the gas and the wave are governing parameters. They also give critical Weber numbers (based on film height) for the onset of atomization. Holowach et al. [11] considered a slightly different mechanism in which aerodynamic drag "pushes" mass from the top of the wave. In their analysis a gas Weber number based on the relative velocity and radius of curvature of the wave is important as well as any parameters needed to determine the drag coefficient. If any part of the gravity force is in line with the drag force then a Bond number based on the liquid density is also important. Lift forces are not considered in their analysis; balancing the forces in that direction would lead to an analysis similar to that of Woodmansee and Hanratty [7].

Finally, atomization as a result of gas-phase structures is considered. Coherent gas-phase vortices may form as a result of injector geometry features such as the gap or the lip in the GCSC injector examined here (see Fig. 2). If the liquid's energy is sufficiently larger than that of the gas then the gas-phase vortex will be displaced; otherwise, the vortex will alter the path of the liquid. In the latter case, droplets may be formed when the vortex distorts and tears liquid away from the film or when aerodynamic forces arising from the new shape of the interface strip liquid away. Simulations reported later in this paper show atomization as a result of liquid moving up the slope of the lip. When the liquid reaches the top of the lip it is sheared off by the oncoming gas (see Fig. 5 to be discussed further below). Gas phase structures in the form of turbulence may also cause atomization in a mode similar to that caused by liquid turbulence provided the gas has sufficient energy.

The value of the kinetic energy ratio or, in other words, a momentum flux ratio, between the liquid and gas determines if gas-phase structures are important. If the liquid has insufficient energy to displace the vortex then it will become entrained by the structure. Important parameters describing atomization are expected to vary with the subsequent droplet producing mechanism. The tearing mechanism is likely described by a Weber number based on recirculation velocity, liquid density and the size of the vortex. A stripping mechanism would involve the parameters cited above for wave stripping. If gas-phase turbulence is important the important parameters would be similar to those for liquid turbulence, but with the gas velocities and diameters relevant to the gas flow.

This examination of potential atomization modes implies that the gas- and liquid-phase Reynolds numbers, Weber number and the momentum flux ratio are likely to be important when describing the film atomization process. As the gas velocity increases, especially relative to the liquid velocity, the dominant cause of atomization moves from liquid turbulence (or no atomization if the liquid is laminar) to aerodynamic stripping to coherent gas-phase structures.

Numerical Simulations

Computational fluid dynamics simulations were performed using FLUENT 6.2 software. Reported here are preliminary results of a planned in-depth study. The geometries for the simulations are given in Fig. 2. Two different injectors were modeled using axially symmetric two-dimensional sections. One injector has a blunt wall which initially separates the two phases; the other has a wall tapered at 25°.
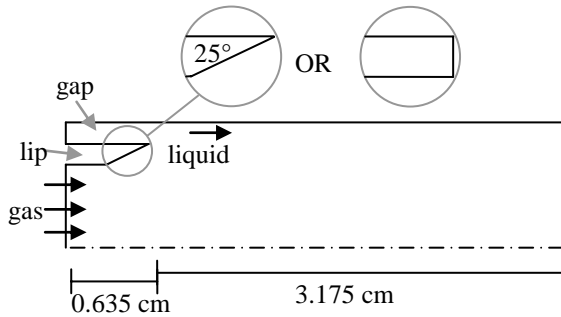
Figure 2. Axisymmetric slice of a gas-centered coaxial-swirl injector. The insets depict the two lip geometries investigated. The gap is 0.165 cm high, the lip is 0.152 cm high and the gas inlet has a radius of 0.635 cm.
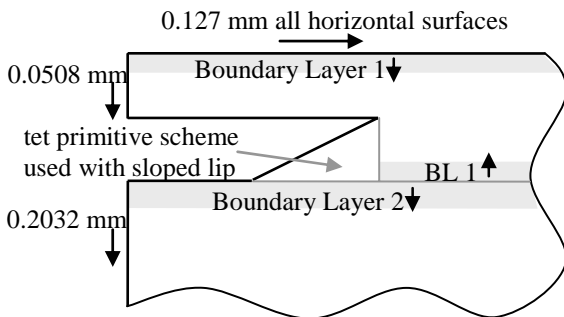

Figure 3. Grid spacing for the simulation. Boundary layer (BL) 1 starts at 0.127 mm and grows at a rate of 0.9091 while Boundary Layer 2 starts at 0.1397 mm and grows at a rate of 1.1.

A quadrilateral grid was used. Fully resolving this flow was not possible due to the sharp gradients created by the existence of a gas-liquid interface and the small size of the droplets produced. Nevertheless, it is hoped the numerical results will give insight and suggest trends, the confirmation of which can be sought experimentally.

Decisions on grid spacing were made with future three-dimensional simulations in mind; the resulting grid should remain a reasonable size when the axisymmetric grid is extended into three dimensions. The axisymmetric grid was fine enough to fully resolve single-phase gas flow in the injector; in other words, the single-phase solution is grid independent. The spacing is given in Fig. 3. Grid points are clustered around the expected interface location. FLUENT tracks the interface using a VOF method with a piece-wise linear reconstruction. A realizable k-ε turbulence model was used for these initial results.

A steady, single-phase solution was developed for the gas by treating the fuel inlet as a wall. The gas inlet condition was fully developed pipe flow at a set mass flow rate, also calculated using FLUENT. The outlet was treated as a constant-pressure boundary at atmospheric pressure; atmospheric pressure was chosen because the complimentary experiments were carried out at that pressure. This gas-phase solution was used as the initial solution for the two-phase simulation.

The fuel was not swirled as in the actual geometry but was instead introduced through the back "wall" of the gap section. The simulations only consider the axial and radial components of the velocity, not the strong tangential velocity actually present in the experiments; this simplification is expected to introduce some errors. The effect of this misalignment should be minimized if the axial velocities are nearly equal in the two cases and the centripetal acceleration of the liquid is somehow considered. The acceleration effects are handled by introducing artificial gravity in the simulations the value of which is based on the calculated tangential velocity at the inlet. The axial velocity was based on a calculated value just after the separating wall. The calculations were based on a constant volume flow rate into and out of the gap section.

Experimental Set-up

Atmospheric tests were conducted using two different atomizers; a diagram of the injector is given in Fig. 1. These geometries are the same as those used in the simulations (Fig. 2) with the addition of a longer gas inlet pipe. The outlet section of the injector, where the liquid and gas come into contact, was constructed of plexiglass to enable imaging of the film. The remainder of the injector was constructed of stainless steel. The design is modular allowing various geometric parameters to be easily altered by replacing individual sections of the assembly. This will allow a wide range of parameterization with minimal hardware costs. To help minimize aberrations and other problems associated with filming through curved surfaces, four flat "viewing windows" were cut into the outlet section of the injector.

The chamber in which the tests were run is essentially a plexiglass box. Two sides of the box have gaps several centimeters high and the width of the box along their top edges. These gaps allow access to the injector during and between runs. The bottom of the chamber has a diffuser to minimize splashing, a drain for the water and side vents through which air is drawn at a low velocity. These air vents help to draw small droplets down and out of the chamber so that it does not fill with mist.

The initial run of tests focused on visualizing the different atomization modes as a function of the gas or liquid flow rates. The affect of tapering the wall separating the gas and liquid was also briefly examined. The operating fluids were gaseous nitrogen and water. The main diagnostic for these tests was backlit photographs taken with a digital camera. In these

preliminary experiments three main points of interest were considered: film length, character of the spray and suggested character of the interface. Approximations of film length and the interface character, i.e. wavy, rough or smooth, are available from the photographs. Spray character was observed and is reported below. The viewing windows were kept clear with gas curtains using shop nitrogen.

The curvature of the injector focuses the backlight which can cause saturation in the central parts of the image. To lessen this effect masking was added to the back window of the injector in a small strip along the centerline. Masking was also added to cover the sections of the window not directly behind the injector.

Results and Discussion
Simulation Results

Results of simulations at two different momentum flux ratios are shown in Figs. 4 and 5. These two simulations show the different behaviors observed in the FLUENT calculations—stripping of hydrodynamic instabilities and atomization due to gas-phase interactions.

In the single-phase flow, prior to the injection of liquid, a vortex forms as the gas flows over the lip. The angle of the cut in the wall is insufficient for the flow to remain attached, but even if the slope was more gentle, a vortex would form as the gas expanded from the lip over the gap region. At low ratios of gas-to-liquid kinetic energy the film displaces this vortex as the liquid exits the gap and a smaller, less energetic recirculation zone is formed. This less energetic vortex does not distort the interface appreciably. If the energy ratio is increased, however, the liquid cannot displace the vortex. The recirculation zone constricts the liquid flow (acting almost like a wall) downstream and the vortex pulls some of the liquid up with it.

The low energy ratio simulations show that waves form on the interface downstream of the lip (see Fig. 4). These waves are very uniform and grow until they reach a size where the gas-flow can strip mass from their crests. The uniform nature and growth of these waves implies that they are caused by hydrodynamic instabilities.

At high energy ratios atomization is completely different. The film thins in the downstream region and increases in thickness, above the gap thickness, near the lip (see Fig. 5). The vortex pulls liquid up along the lip. When liquid reaches the top of the lip it is sheared off as it is subjected to cross flow. In the simulations the amount of liquid under the recirculation zone increases until a certain critical point is reached. At this point the vortex is pushed downstream by the liquid and a mass of liquid moves downstream with it, thinning and distorting as the film is subjected to the circulation of

the vortex and the higher velocity of the main gas stream.

The lip seems to have very little effect on the general atomization behavior as evidenced in Figs. 5 and 6. A stronger impact is expected if the gradient of the taper is small enough that the flow remains attached. Adding artificial gravity to mimic some effects of the centripetal acceleration also produces little change in the general atomization behavior. Gravity alters the early behavior of the film, keeping it close to the wall (see Figs. 5 and 6). The atomization of the developed film is qualitatively similar with and without gravity at the conditions examined, however. The bounding conditions for the different modes should be affected by the both lip shape and inclusion of the gravity; however, the operating conditions presented here were chosen to be far from the boundaries.

Experimental Results

Two sets of experiments were run with each injector. Either the gas flow rate was held constant while the liquid flow rate was increased in increments or the liquid flow rate was constant while the gas flow rate increased (see Table 1). Photographs and other visual evidence suggest that the atomization modes of the two injectors were similar; the difference mainly being limited to the operating conditions at which the atomization modes change. Figures 7 and 8 show a selection of photographic results, which are described in further detail below and in Table 1. The pictures are annotated for clarity: A is the actual outer edge of the injector, B is a reflection of the outer edge (not always visible) and C is a reflection from the liquid-gas interface. As the film length decreases the length of the light line C also decreases. D denotes the edge of the plexiglass, E is at the end of the lip and F is the injector outlet. The water seen extending beyond the outlet is liquid adhering to the wide outlet face of the injector and does not represent a sheet or atomized droplet. In some images waves or changes in the roughness of the interface are evident; these characteristics are somewhat faint and do not reproduce, i.e. print, clearly; consequently, Table 1 briefly describes the character of the interface at different flow rates as well as succinctly describing the spray.

Figure 7 shows a series of experiments where the gas flow rate is held constant while the liquid flow rate is increased in increments of 0.3785 liter/min (0.1 gal/min). At very low liquid flow rates the film is quite short. Droplets wetting the plexiglass downstream can be seen to travel upstream due to the vortex caused by the separated gas flow. As the liquid flow is increased the film length increases. The general profile of the film resembles the simulations at high kinetic energy ratios with the film being thinned in the downstream direction (see Fig. 5). If the flow rate is increased

Figure 4. Axisymmetric simulation of the injector with a gas flow rate of 0.014 kg/s and an axial liquid velocity of 3.47 m/s. The black region represents the liquid. The flow is fully developed; images are given at $1.0x10^{-4}$ s intervals from left to right and top to bottom. The simulation shown without artificial gravity is shown to better illustrate the stripping phenomenon.
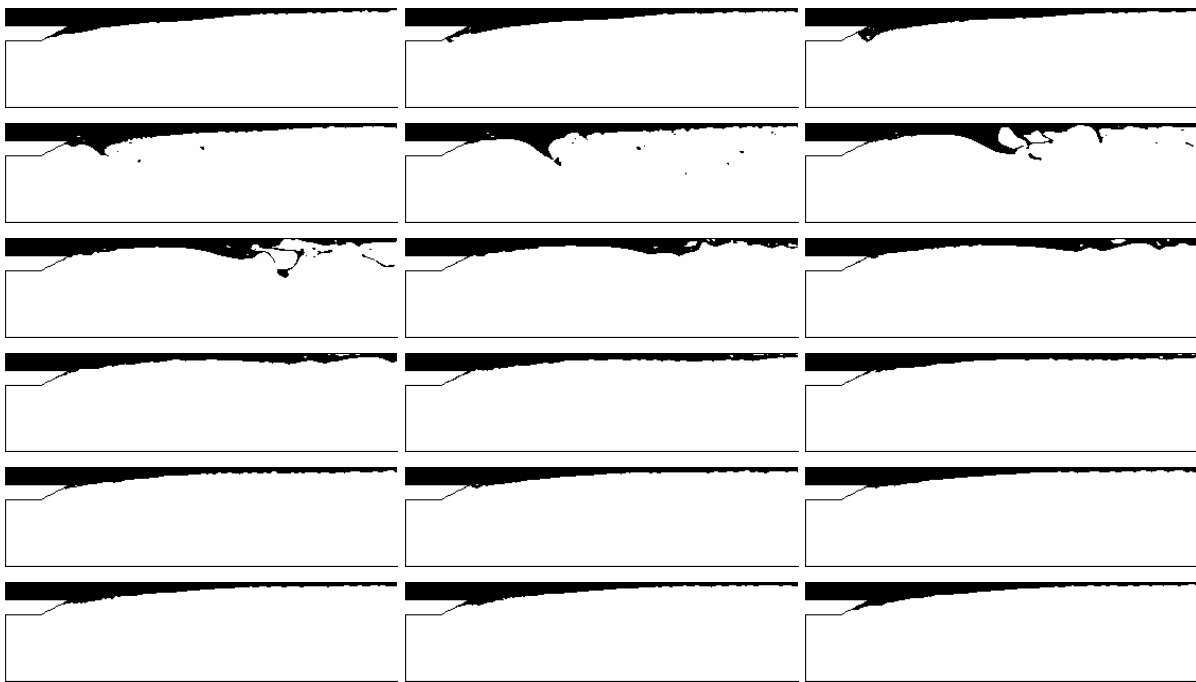

Figure 5. Axisymmetric simulation of the injector with a gas flow rate of 0.014 kg/s and an axial liquid velocity of 0.347 m/s. The black region represents the liquid. The flow is fully developed and images are given at $1.5x10^{-3}$ s intervals from left to right, top to bottom.
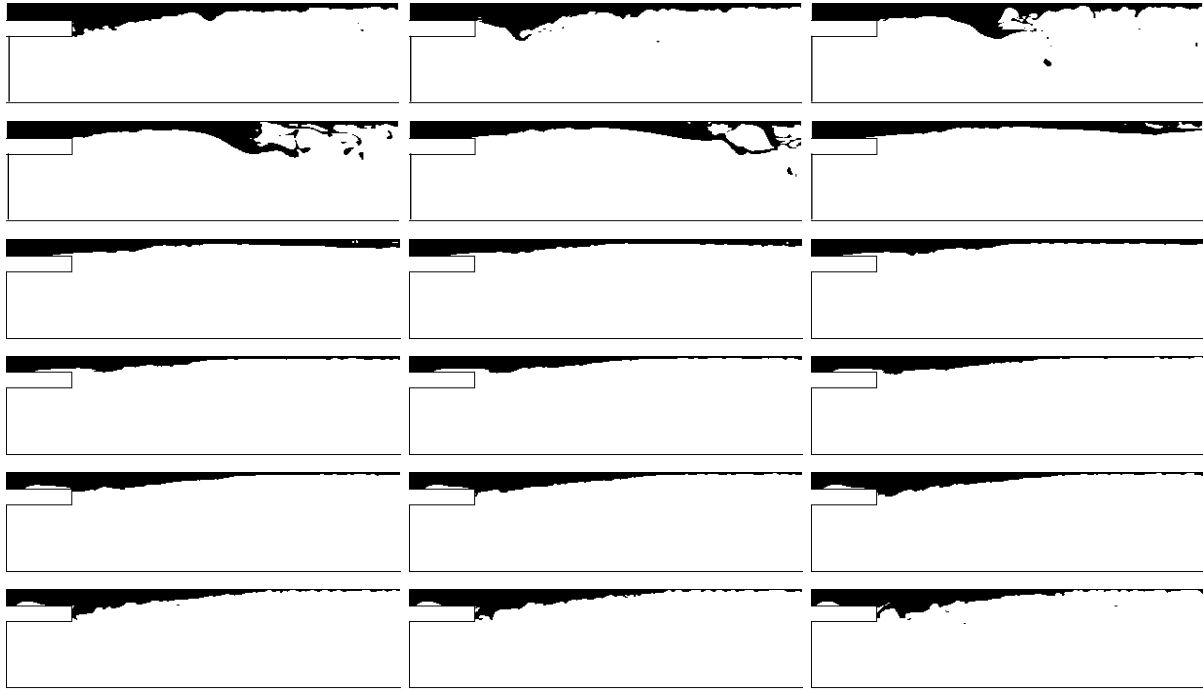
Figure 6. Axisymmetric simulation of the injector with a gas flow rate of 0.014 kg/s and an axial liquid velocity of 0.347 m/s. The black region represents the liquid. The flow is fully developed and images are given at 1.5×10^{-3} s intervals from left to right, top to bottom.

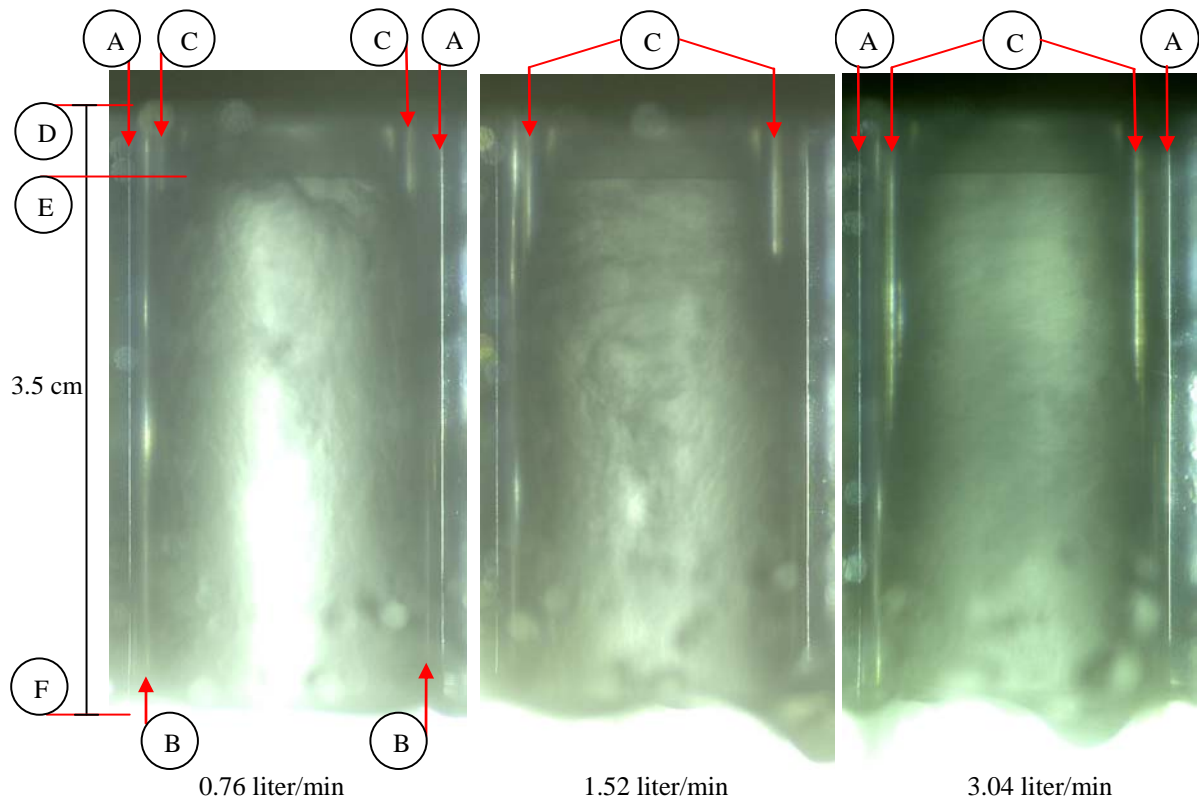0.76 liter/min   1.52 liter/min   3.04 liter/min

Figure 7. Selected photographs with a gas flow rate of 0.045 kg/s and liquid flow rates as indicated. The annotated features are the outer edge of the injector (A), a reflection of this edge (B), a reflection from the liquid-gas interface (C), the edge of the plexiglass (D), the lip end (E) and the injector outlet (F).

Figure 8. Selected photographs with a liquid flow rate of 2.74 liter/min and liquid flow rates as indicated. The annotated features are the outer edge of the injector (A), a reflection of this edge (B), a reflection from the liquid-gas interface (C), the edge of the plexiglass (D), the lip end (E) and the injector outlet (F).
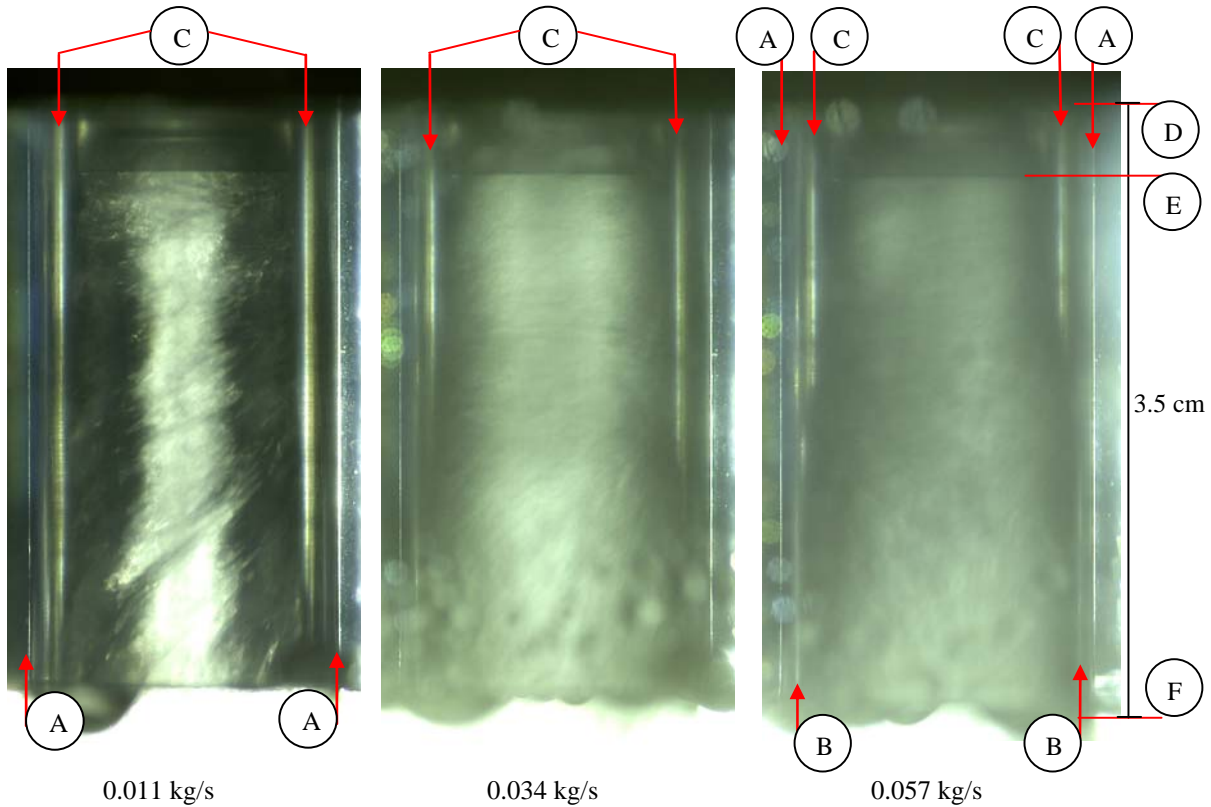
| Liquid flow rate liter/min (gal/min)	Gas flow rate kg/s (lb$_m$/s)	Spray Character	Interface Character
2.74 (0.725)	0.000 (0.000)	conic sheet creates hollow cone spray	regular waves oriented at some angle to the mean gas flow
2.74 (0.725)	0.011 (0.025)	partial sheet with narrower cone angle; swirl very evident	regular waves oriented at some angle to the mean gas flow throughout most/all of film
2.74 (0.725)	0.023 (0.050)	many large droplets, possibly some ligaments at the exit	regular waves at some angle throughout most/all film
2.74 (0.725)	0.034 (0.075)	large droplets on periphery of spray; medium-fine center spray	regular waves at some angle throughout most/all film
2.74 (0.725)	0.045 (0.100)	as above, less large droplets slightly finer spray	rough, possible waves oriented perpendicular to gas flow
2.74 (0.725)	0.057 (0.126)	as above, very few large droplets	rough
2.74 (0.725)	0.068 (0.150)	no large droplets	rough
0.76 (0.200)	0.045 (0.100)	very fine mist	film too short to characterize
1.14 (0.300)	0.045 (0.100)	somewhat coarser, but still fine	rough and still quite short
1.52 (0.402)	0.045 (0.100)	slightly coarser than above	rough, possible waves oriented perpendicular to gas flow
1.88 (0.498)	0.045 (0.100)	slightly coarser than above	rough, possible waves oriented perpendicular to gas flow
2.27 (0.601)	0.045 (0.100)	a few large droplets appear on edge of spray	rough, possible waves downstream, oriented at angle to gas flow
3.04 (0.803)	0.045 (0.100)	increased number of large droplet, coarser spray	regular waves at some angle throughout most/all film
3.41 (0.900)	0.045 (0.100)	partial sheet; swirl very evident	regular waves at some angle throughout most/all film
Table 1. Character of spray and interface at various flow rates			
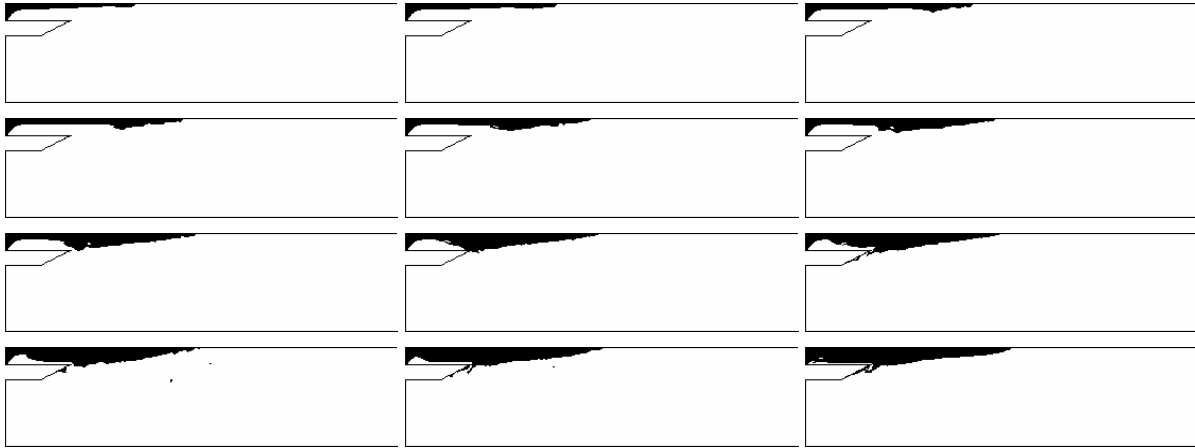
Figure 9. Axisymmetric simulation of the injector with a gas flow rate of 0.014 kg/s and an axial liquid velocity of 0.347 m/s showing the initial behavior wherein a bubble is temporarily formed. The black region represents the liquid. The images are given at 3.0×10^{-3} s intervals from left to right and top to bottom.

further the film reaches the end of the injector before it is atomized. As it has nears the end the average droplet size increases as large droplets are periodically ripped from the edge of the injector. Past a certain liquid flow rate, regular waves appear on the surface of film. These waves are likely due to hydrodynamic instabilities. When visible they clearly show the swirl in the fluid as they are oriented at some angle.

The liquid flow rate is held constant while the gas flow rate is increased in Fig. 8. With no gas flow the injector behaves as a traditional pressure-swirl atomizer creating a conic sheet at the exit. As the gas flow is increased the sheet length decreases until no sheet is visible. When a sheet is formed at low gas flow rates, the cone angle is very sensitive to the gas flow rate; it decreases rapidly as the flow is increased. When the sheet disappears regular waves are still visible on the surface of the film. The film shortens and the waves become less evident or disappear as the gas flow increases further. At these flow rates the film behavior is largely dictated by the gas-phase structure. Eventually, the surface of the liquid becomes turbulent and appears cloudy due to the scatter off the roughened surface; this interface turbulence is caused by gas-phase turbulence interacting with the film surface.

At very low liquid flow rates the gap does not fill completely. Beyond a certain flow rate the gap is generally filled, but can be susceptible to bubble formation. The simulations hint at the process by which this bubble forms as illustrated in Fig. 9. At start-up the simulations show the film filling only the back portion of the gap. Centripetal forces keep the film thin and against the wall as it begins to flow downstream. The recirculation vortex creates what is essentially a wall restricting the film's thickness. At some point downstream this "wall" is close enough to

the actual wall that it restricts the film flow. Consequently, liquid builds up pressing the artificial "wall" outward. The simulations show that the film initially thickens near the restriction point, i.e. at its downstream edge. The point where the film begins to widen moves upstream. Eventually, the film is thick enough to reach the underside of the lip; this occurs before the upstream part of the film has fully filled the gap area resulting in a bubble (see Fig. 9). In the simulations the bubble is forced out as the gap fills, but in the experiments gas sometimes becomes trapped in the gap area and bubbles can be seen circulating with the swirling fluid.

When the gas velocity is low, the momentum of the incoming liquid does not fully spread from the four inlets despite forming a continuous film. At some operating conditions four distinct jets of liquid are formed downstream of the injector exit. With no gas flow the injector forms an intact sheet with no evidence of distinct inlets, but as the gas flow is increased the sheet narrows, shortens and suddenly separates into four distinct jets. As the gas flow is further increased and aerodynamic effects became more important, the bias appears to dissipate. The exact reasons for this behavior remain under investigation, but the current understanding suggests that, despite forming an intact film, the streams have a finite mixing length greater than the injector length. With no gas flow the sheet has a sufficient length to allow mixing to occur and when the aerodynamic effects are sufficiently large they increase the mixing so that a shorter length is needed. In the interim, however, mixing is incomplete and the inlet streams maintain some individual identity.

Discussion

Comparisons between the general character of the film in experiments and axisymmetric simulations are

promising. Both show two modes of atomization—one characterized by hydrodynamic instabilities and one dominated by the recirculation zone in the gas. It is recognized that better agreement can be achieved by extending the model to three dimensions. Three-dimensional simulations will capture the true acceleration field and other swirl-related effects as well as allowing better matching of the actual inlet conditions. Yet by judiciously selecting the operating conditions for the simulations, useful results have been obtained. The current understanding suggests that the relative momentum difference between the liquid and gas, particularly in the axial direction, plays a large role in the film's behavior, so comparisons of the simulations and experiments are based on equating the calculated average axial velocity of the liquid at the end of the lip (densities are fixed in these atmospheric tests). The results show that capturing the axial liquid velocity allows similar film behavior to be captured. The contribution of the tangential velocity to the general character of atomization is considered to be largely through centripetal acceleration; consequently, the simulations introduce an artificial, constant gravity to help account for the tangential velocity. Including gravity allows the simulations to capture a bubble-formation mechanism helping to explain the bubbles observed in the experiments.

The conditions for the simulations were chosen based on geometric scaling of similar earlier GCSC injectors [2] with the gas-liquid relationship scaled through the momentum flux ratio. The simulations appear to show effective atomization, as expected. When the experimental apparatus was run at these conditions, however, film atomization did not occur. The quality of atomization in the experiments suggests that kinetic energy ratio may not be the most appropriate scaling parameter or, at least, that it must account for the velocity direction. Additionally, the discussion of atomization regimes suggests that some sort of Weber number scaling is likely to be more effective than geometric scaling. Scaling is further complicated by a change in geometry between the injector that was the basis for scaling and the current injector. To aid understanding of GCSC injectors a sheltering gap, i.e. shroud, was added so that the film was developed prior to exposure to the gas. Previous injector work at Edwards AFB, from which the scaling was based, did not include this gap.

Conclusions and Future Work

Preliminary experimental and numerical studies of gas-centered swirl-coaxial injectors show two main types of atomization behavior. These behaviors were anticipated from earlier studies of the literature. At high kinetic energy ratios gas-phase structures control the film's behavior and atomization. At low (and zero)

kinetic energy ratios waves form on the surface of the film and are responsible for atomization. The experiments also showed atomization due to turbulence, but this occurred at relatively large gas velocities suggesting that the gas turbulence, not the liquid's turbulence, was responsible. Scaling of prior similar injectors based on the kinetic energy ratio suggests, however, that this ratio may not be the best choice. The results indicate that, the scaling must somehow account for the velocity vectors.

The work presented here is the beginning of a more involved effort to develop effective design criteria for GCSC injectors through an understanding of their atomization mechanics. Plans include developing an understanding of the bounds of each atomization regime. Additionally, the important nondimensional parameters describing each regime need to be better understood. To achieve these goals a further physical understanding of these regimes is needed. Simple physical models suggest potentially important nondimensional parameters; these models will be further investigated and extended as needed. Additional experiments are planned including some parametric studies and measurements of important atomization quantities. High-speed images and laser sheet illumination are planned for these experiments. Expanded numerical studies are also planned, including moving to three-dimensional simulations. Simulations allow us to change parameters not as easily altered in experiments. They can also generate more data on certain quantities, such as character of the turbulence.

References
1. Canino, J., Heister, S., Sankaran, V. and Zakharov, S., *41st AIAA/ASME/SAE/ASEE Joint Propulsion Conference and Exhibit*, Tucson, AZ, July 10-13, 2005.
2. Strakey, P.A., Cohn, R.K, and Talley, D.G., *17th ILASS Americas*, Arlington, VA, 16-19 May 2004.
3. Khavkin, Y., *Atomization and Sprays* 11:757-774 (2001).
4. Sarpkaya, T. and Merrill, C.F., *AIAA Journal* 39:1217-1229 (2001).
5. Okawa, T., Kotani, A. and Kataoka, I., *International Journal of Heat and Mass Transfer* 48:585-598 (2005).
6. Lightfoot, M.D.A., *19th ILASS-Americas*, Toronto, Canada, May 23-26, 2006.
7. Woodmansee, D.E. and Hanratty, T.J., *Chemical Engineering Science* 24:299-307 (1969).
8. Dai, Z., Chou, W.H. and Faeth, G.M., *Physics of Fluids* 10:1147-1157 (1998).
9. Liao, Y., Jeng, S.M., Jog, M.A. and Benjamin, M.A., *Journal of Propulsion and Power* 17:411-417 (2001).

10. Yecko, P., *16th ILASS Americas*, Monterey, CA, May 18-21, 2003.
11. Holowach, M.J., Hochreiter, L.E. and Cheung, F.B., *International Journal of Heat and Fluid Flow* 23:807-822 (2002).